

Audio-Visual Speech Enhancement based on Multimodal Deep Convolutional Neural Network

Jen-Cheng Hou¹, Syu-Siang Wang², Ying-Hui Lai³, Jen-Chun Lin⁵, Yu-Tsao¹, Hsiu-Wen Chang⁴ and Hsin-Min Wang⁵

¹Research Center for Information Technology Innovation, Academia Sinica, Taiwan

²Graduate Institute of Communication Engineering, National Taiwan University, Taiwan

³Department of Electrical Engineering, Yuan Ze University, Taiwan

⁴Department of Audiology and Speech Language Pathology, Mackay Medical College, Taiwan

⁵Institute of Information Science, Academia Sinica, Taiwan

{coolkiu, yu.tsao}@citi.sinica.edu.tw, d02942007@ntu.edu.tw, yhlai@ee.yzu.edu.tw, hsiuwen@mmc.edu.tw, whm@iis.sinica.edu.tw

Abstract

Speech enhancement (SE) aims to reduce noise in speech signals. Most SE techniques focus on addressing audio information only. In this work, inspired by multimodal learning, which utilizes data from different modalities, and the recent success of convolutional neural networks (CNNs) in SE, we propose an audio-visual deep CNN (AVDCNN) SE model, which incorporates audio and visual streams into a unified network model. In the proposed AVDCNN SE model, audio and visual features are first processed using individual CNNs, and then, fused into a joint network to generate enhanced speech at an output layer. The AVDCNN model is trained in an end-to-end manner, and parameters are jointly learned through back-propagation. We evaluate enhanced speech using five objective criteria. Results show that the AVDCNN yields notably better performance as compared to an audio-only CNN-based SE model, confirming the effectiveness of integrating visual information into the SE process.

Index Terms: multimodal learning, speech enhancement, audio-visual learning, deep convolutional neural network

1. Introduction

The primary goal of speech enhancement (SE) is to improve the intelligibility and quality of noisy speech signals by reducing the noise components of noise-corrupted speech. To attain satisfactory performance, SE has been used as a fundamental unit in different speech-related applications, such as automatic speech recognition [1–3], speaker recognition [4, 5], speech coding [6, 7], hearing aids [8, 9], and cochlear implant [10, 11]. In the past few decades, numerous and diverse SE methods have been proposed and proven to provide improved sound quality. One notable approach, i.e., spectral restoration, estimates a gain function (based on the statistics of noise and speech components), which is then used to suppress noise components in a frequency domain to obtain a clean speech spectrum from a noisy speech spectrum [12–16]. In recent years, SE methods based on deep learning have been proposed and investigated in detail, such as a denoising autoencoder [17, 18]. A deep neural network (DNN)-based SE method exhibits better performance than a conventional SE model [19, 20]. In addition, inspired by the success of image recognition using convolutional neural networks (CNNs), a CNN-based model has been shown to

obtain good results in SE owing to its strength in handling 2-D structured input [21, 22].

In addition to speech signals, visual information is important in human-human or human-machine interaction. A study of the McGurk effect [23] indicated that the motion of the mouth or lips could play an important role in speech processing. Accordingly, audio-visual multimodality has been adopted in numerous fields of speech-processing [24–28]. These results showed that visual modality enhances the performance of speech processing, as compared to its counterpart that uses only audio modality. Recently, we have proposed integration of audio and visual information for SE [29]. In that work, Mel filter banks and the Gauss–Newton deformable part model [30] were used to extract audio and mouth shape features. Experimental results showed that the performance of a DNN with audio-visual inputs was better than that of a DNN with only audio inputs in standardized objective evaluations. In the present work, audio and visual streams are processed using individual networks based on CNNs. The outputs of the two networks are fused into a joint network. The entire model is trained in an end-to-end manner and structured as an audio-visual encoder-decoder network. More specifically, noisy speech and visual data are placed at inputs, and clean speech and visual data are placed at outputs. Notably, the visual information at output serves as a part of the constraints during the training of the model, and thus, the system is a multi-task learning system that considers heterogeneous information. Such audio-visual encoder-decoder network design has not been adopted in related works [29, 31]. Experimental results show that the proposed audio-visual SE model is capable of outperforming two other baseline models in terms of several standard evaluation metrics, including perceptual evaluation of speech quality (PESQ) [32], short-time objective intelligibility (STOI) [33], speech distortion index (SDI) [34], hearing-aid speech quality index (HASQI) [35], and hearing-aid speech perception index (HASPI) [36], confirming the effectiveness of incorporating visual information into the CNN-based multimodal SE framework.

The rest of this paper is organized as follows: Section 2 describes feature extraction and preprocessing in audio and visual streams. Section 3 introduces the proposed CNN-based audio-visual model for SE and describes two baseline models for comparison. Section 4 describes the experimental setup and results, and section 5 provides the concluding remarks of this study.

2. Datasets and preprocessing

In this section, we provide the details of datasets and preprocessing for audio and visual streams.

2.1. Data collection

The prepared datasets contain video recordings of 320 utterances of Mandarin sentences spoken by a native speaker. The length of each utterance is approximately 3–4 seconds. The utterances were recorded in a quiet room with sufficient light, and the speaker was filmed from the front view. Videos were recorded at 30 frames per second (fps) at a resolution of 1920 pixels \times 1080 pixels. Stereo audio channels were recorded at 48 kHz. One-fourth of the corpus (40 utterances) was randomly selected as a testing set, with the remaining 280 utterances used as training sets.

2.2. Audio feature extraction

We resampled an audio signal at 16 kHz and used only a mono channel for further processing. Speech signals were converted into a frequency domain and processed into a sequence of frames using the short-time Fourier transform. Each frame window was 32 milliseconds and window overlap ratio was 37.5%. For each speech frame, we extracted the logarithmic power spectrum and normalized the amplitude by removing mean and dividing by standard deviation. We concatenated ± 2 frames to the central frame as context windows. Accordingly, audio features had dimensions of 257×5 at each time step. We use X and \hat{Y} to denote noisy and clean speech features, respectively.

2.3. Visual feature extraction

For the visual stream, we converted each video, which contained an utterance, into image sequences at a fixed frame rate of 50 fps. Next, we detected the mouth using the Viola–Jones method [37], resized the cropped mouth region to 16 pixels \times 24 pixels, and retained its RGB channels. In each channel, we rescaled image pixel intensities in a range of 0 to 1. We subtracted mean and divided by standard deviation for normalization. In addition, we concatenated ± 2 frames to the central frame, resulting in visual features having dimensions of $80 \times 24 \times 3$ at each time step. We use \hat{Z} to represent input visual features.

2.4. Audio-visual synchronization

As mentioned above, audio and visual streams were processed into a sequence of features at the same frame rate. Owing to the different sampling rates of the audio and visual streams, the time duration at each stream could not exactly match for the same video, resulting in a different number of frames in the audio and visual streams. This out-of-sync error could be detected by a viewer, and the threshold for detection was approximately 45 milliseconds when sound advanced with respect to vision [38]. For the datasets that we used in this study, once the number of frames did not match, the visual stream always outnumbered the audio stream, where the maximum difference was 4 frames. Accordingly, we considered the issue of unequal number of frames as an acceptable time mismatch in this work. To overcome the issue, we trimmed the longer sequence of frames to make the number of frames identical at the audio and visual features for each video. In audio-visual speech recognition, a method based on coupled hidden Markov models is adopted to address the asynchrony between audio and visual streams [26].

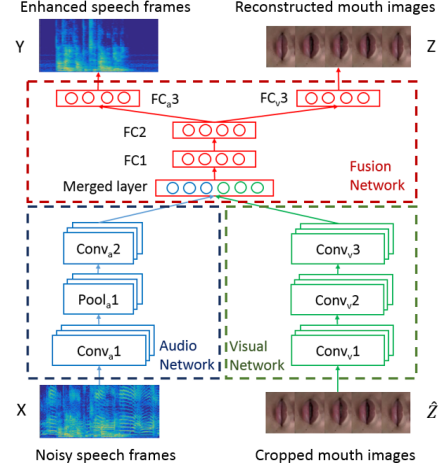


Figure 1: Architecture of the proposed AVDCNN.

3. Audio-visual deep convolutional neural network (AVDCNN)

The model architecture of the proposed AVDCNN is shown in Figure 1. It is composed of two individual networks that handle audio and visual streams (Audio Network and Visual Network). The outputs at each network are fused into a fusion network (Fusion Network). The CNN, maximum pooling layer, and fully-connected layer in the diagram are abbreviated as Conv_a1, Conv_a2, Conv_v1, ..., Pool_a1, FC1, FC2, FC_a3, and FC_v3, where subscripts 'a' and 'v' denote the audio and visual stream, respectively. In the following section, we describe the training procedure of the AVDCNN.

3.1. Training the AVDCNN model

To train the AVDCNN model, we first prepare noisy-clean speech pairs and mouth images. As described in sections 2.2 and 2.3, we have the logarithmic amplitudes of noisy (X) and clean (\hat{Y}) spectra and the corresponding visual features (\hat{Z}). For each time step, we obtain the output of Audio Network as

$$A_i = \text{Conv}_a2 \left(\text{Pool}_a1 \left(\text{Conv}_a1(X_i) \right) \right), i = 1 \dots K \quad (1)$$

where K is the number of training samples. The output of Visual Network is

$$V_i = \text{Conv}_v3 \left(\text{Conv}_v2 \left(\text{Conv}_v1(\hat{Z}_i) \right) \right), i = 1 \dots K \quad (2)$$

Next, we flatten A_i and V_i , and then, concatenate the two features as the input of Fusion Network, $F_i = [A_i' \ V_i']'$. A feed-forward cascaded fully-connected network is computed as follows:

$$Y_i = \text{FC}_a3 \left(\text{FC}_2 \left(\text{FC}_1(F_i) \right) \right), i = 1 \dots K \quad (3)$$

$$Z_i = \text{FC}_v3 \left(\text{FC}_2 \left(\text{FC}_1(F_i) \right) \right), i = 1 \dots K \quad (4)$$

The parameters of the AVDCNN, denoted by θ , are randomly initialized from -1 to 1 and are jointly trained by optimizing the following objective function using back-propagation:

$$\min_{\theta} \left(\frac{1}{M} \sum_{m=1}^M \|Y_m - \hat{Y}_m\|_2^2 + \|Z_m - \hat{Z}_m\|_2^2 \right) \quad (5)$$

where M is the number of training samples.

Stride size of 1×1 is used in the CNN parts of the AVDCNN and a dropout of 0.1 is adopted after FC1 and FC2 to prevent overfitting. Batch normalization is applied for each layer in the model. Other configurations are shown in Table 1.

Table 1: *Configurations of the AVDCNN model.*

Layer Name	Kernel	Activation Function	Number of Filters or Neurons
Conv _a 1	12×2	Linear	10
Pool _a 1	2×1		
Conv _a 2	5×1	Linear	4
Conv _v 1	15×2	Linear	12
Conv _v 2	7×2	Linear	10
Conv _v 3	3×2	Linear	6
Merged Layer			2804
FC1		Sigmoid	1000
FC2		Sigmoid	800
FC _a 3		Linear	600
FC _v 3		Linear	1500

3.2. Using the AVDCNN model for speech enhancement

In the testing phase, the logarithmic amplitudes of noisy speech signals and the corresponding visual features are fed into the trained AVDCNN model to obtain the logarithmic amplitudes of enhanced speech signals and visual features as outputs. Similar to spectral restoration approaches, the phases of noisy speech are borrowed as phases for enhanced speech. Then, the AVDCNN-enhanced amplitudes and phase information are used to synthesize enhanced speech. We consider the visual features at the output of the trained AVDCNN only as auxiliary information and do not use it for evaluating enhanced results.

3.3. Baseline models

In this work, we compare the proposed AVDCNN model with two baseline models. The first is an audio-only deep CNN (ADCNN) and the second is an audio-visual DNN (AVDNN). The ADCNN model disconnects any visual-related parts in the AVDCNN with the same configurations, as shown in Figure 2. The AVDNN is an audio-visual SE model that we proposed in [28], which is primarily based on DNN architecture without visual constraints at the output during training.

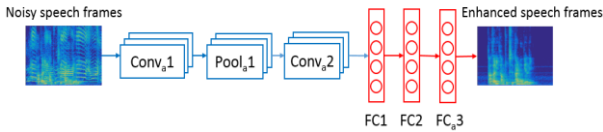


Figure 2: *Architecture of the ADCNN model, which is the model in Figure 1 with visual parts disconnected.*

4. Experiments and results

4.1. Experimental setup

In this section, we describe the evaluation of the proposed AVDCNN model using a speech enhancement task. To prepare the clean-noisy speech pairs, we use three different source noises including baby crying sounds, car engine noise, and two talkers (two talkers speaking in the background). Next, we generate different signal-to-noise ratios (SNRs) for training sets (-6 dB, -2 dB, 2 dB, 6 dB, 10 dB) and testing sets (-5 dB, 0 dB, 5 dB). The noise sources used in the training and testing phases

are matched. We use Adam [39] as the learning algorithm for the training method, with an initial learning rate of 0.001. We stop training when 10 epochs exhibit no improvement.

4.2. Comparison of spectrogram

In Figure 3, parts (a), (b), (c), (d), and (e) demonstrate the spectrograms of clean speech, noisy speech mixed with baby crying sounds (at 0 dB SNR), and speech enhanced by the AVDCNN, ADCNN, and AVDNN, respectively. We note that noise components (the baby crying sounds in the background) are clearly removed in (c), (d), and (e), showing the effectiveness of these three models. In addition, we observe that detailed structures from AVDCNN-enhanced speech can be preserved better than in other baseline models, as shown in the red frame in Figure 3. In the following section, we provide more objective evaluations on the enhanced results of these models.

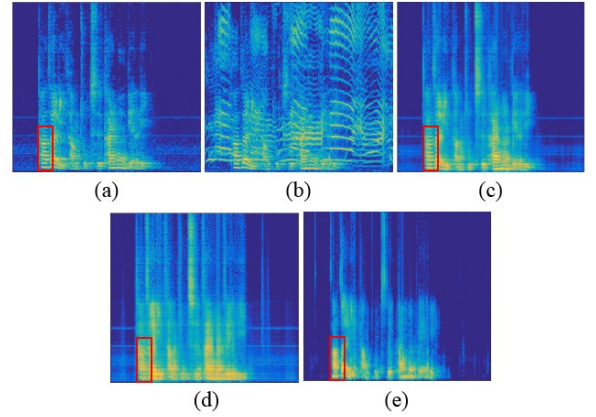


Figure 3: *Comparison of spectrograms. (a) clean speech (b) noisy speech (baby crying) at 0 dB SNR (c) speech enhanced by AVDCNN (d) speech enhanced by ADCNN and (e) speech enhanced by AVDNN.*

4.3. Objective results

We use five objective metrics as evaluation methods, including PESQ, STOI, SDI, HASQI and HASPI. The PESQ score ranges from 0.5 to 4.5. A higher score implies that enhanced speech is closer to clean speech. STOI shows the intelligibility measurement of enhanced speech. SDI calculates the extent of distortion between clean and enhanced speech, with lower SDI indicating a smaller difference between clean and enhanced speech signals. HASQI and HASPI scores represent speech quality and intelligibility in case of wearing hearing aids. For each evaluation method, we report the average scores of the 40 test utterances. Except for SDI, larger values are better for all other scores.

Figures 4, 5, and 6 show the average PESQ, STOI, and SDI scores (over three different noises) of enhanced speech obtained using different models at -5 dB, 0 dB, and 5 dB SNRs, respectively. Tables 2 and 3 report the detailed HASQI and HASPI scores of noisy and enhanced speech. To demonstrate the benefit of fusing visual stream, we compare the two CNN-based models and it is observed that AVDCNN outperforms ADCNN in each evaluation criteria, showing the effectiveness of incorporating visual information to achieve even better SE performance. Next, we note that the CNN-based models (AVDCNN) consistently outperform DNN-based model (AVDNN), confirming CNN as an effective learning framework for the audio-visual SE task.

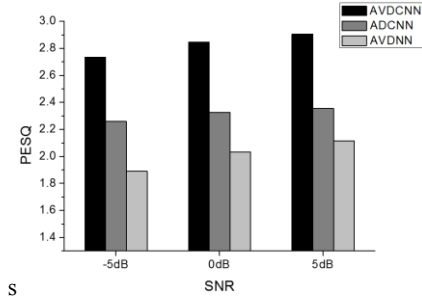


Figure 4: Mean PESQ scores (over three noise types) of enhanced speech for different models under different SNRs.

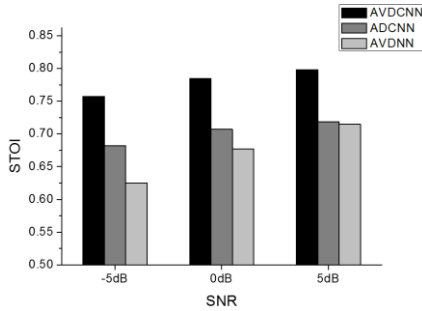


Figure 5: Mean STOI scores (over three noise types) of enhanced speech for different models under different SNRs

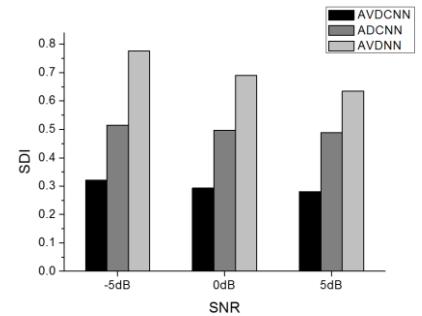


Figure 6: Mean SDI scores (over three noise types) of enhanced speech for different models under different SNRs.

Table 2: HASPI scores of noisy and enhanced speech for different models under different noises.

SNR	-5dB	0dB	5dB
Noisy(baby crying)	0.1156	0.1517	0.2201
AVDNN	0.1586	0.2020	0.2372
ADCNN	0.3562	0.4003	0.4347
AVDCNN	0.4872	0.5294	0.5612
Noisy(car engine)	0.1133	0.1674	0.2347
AVDNN	0.1683	0.2231	0.2619
ADCNN	0.3777	0.4356	0.4673
AVDCNN	0.5289	0.5651	0.5856
Noisy(2 talkers)	0.0439	0.0810	0.1407
AVDNN	0.1251	0.1671	0.2075
ADCNN	0.4109	0.4418	0.4549
AVDCNN	0.4797	0.5175	0.5364

Table 3: HASPI scores of noisy and enhanced speech for different models under different noises.

SNR	-5dB	0dB	5dB
Noisy(baby crying)	0.7417	0.8288	0.9402
AVDNN	0.8522	0.9192	0.9620
ADCNN	0.9890	0.9937	0.9965
AVDCNN	0.9982	0.9988	0.9992
Noisy(car engine)	0.7327	0.8815	0.9556
AVDNN	0.8963	0.9608	0.9794
ADCNN	0.9936	0.9970	0.9979
AVDCNN	0.9988	0.9992	0.9993
Noisy(2 talkers)	0.2051	0.4668	0.7509
AVDNN	0.7400	0.8893	0.9408
ADCNN	0.9954	0.9968	0.9973
AVDCNN	0.9983	0.9988	0.9990

4.4. Reconstructed mouth images

In the proposed AVDCNN system, we use visual input as an auxiliary clue for speech signals and add visual information at output as a part of the constraints during the training of the model. Therefore, the proposed system is actually an audio-visual encoder-decoder system with multi-task learning. In addition to enhanced speech frames, we receive the corresponding mouth images at the output in the testing phase. It is interesting to investigate the images obtained using the audio-visual encoder-decoder system. Figure 7 shows a few visualized samples. For now, we simply view these images as a “by-product” of the audio-visual system, as compared to the target enhanced speech signals. However, in future, it will be interesting to explore the lip motions that the model can learn when the corresponding fed visual hints are considerably corrupted or not provided.

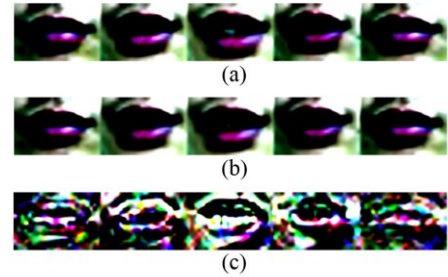


Figure 7: Visualizing the normalized mouth images. (a) Visual input and (b) visual output of the proposed AVDCNN model. (c) Difference between (a) and (b), with amplitude magnified ten times.

5. Conclusions

In this paper, we have proposed a novel CNN-based audio-visual encoder-decoder system with multi-task learning, called AVDCNN. The model utilizes individual networks to process input data with different modalities, and a fusion network is followed to learn joint multimodal features. We train the model in an end-to-end manner. The experimental results obtained using the proposed architecture show that its performance in SE task is better than that of two baseline models for five objective evaluation methods, confirming the effectiveness of integrating visual information into the SE process. In future, we will attempt to improve the proposed architecture by integrating well-trained networks at audio or visual feature description or modifying objective functions to capture better cross-modal relations.

6. References

- [1] J. Li, L. Deng, R. Haeb-Umbach, and Y. Gong, *Robust Automatic Speech Recognition: A Bridge to Practical Applications*, 1st ed. Academic Press, 2015.
- [2] T. Virtanen, R. Singh, and B. Raj, *Techniques for noise robustness in automatic speech recognition*, John Wiley & Sons, 2012.
- [3] B. Li, Y. Tsao, and K. C. Sim, "An investigation of spectral restoration algorithms for deep neural networks based noise robust speech recognition," in *Proc. INTERSPEECH*, 2013, pp. 3002-3006.
- [4] A. El-Solh, A. Cuhadar, and R. A. Goubran, "Evaluation of speech enhancement techniques for speaker identification in noisy environments," in *Proc. ISMW*, 2007, pp. 235-239.
- [5] J. Ortega-Garcia and J. Gonzalez-Rodriguez, "Overview of speech enhancement techniques for automatic speaker recognition," in *Proc. ICSLP*, vol. 2. 1996, pp. 929-932.
- [6] J. Li, L. Yang, Y. Hu, M. Akagi, P.C. Loizou, J. Zhang, and Y. Yan, "Comparative intelligibility investigation of single-channel noise reduction algorithms for Chinese, Japanese and English," *Journal of the Acoustical Society of America*, vol. 129, no. 5, pp. 3291-3301, 2011.
- [7] J. Li, S. Sakamoto, S. Hongo, M. Akagi, and Y. Suzuki, "Two-stage binaural speech enhancement with Wiener filter for high-quality speech communication," *Speech Communication*, vol. 53, no. 5, pp. 677-689, 2011.
- [8] T. Venema, *Compression for Clinicians*, 2nd ed. Thomson Delmar Learning, 2006, ch. 7.
- [9] H. Levitt, "Noise reduction in hearing aids: an overview," *J. Rehabil. Res. Dev.*, vol. 38, no. 1, pp.111-121, 2001.
- [10] Y.-H. Lai, F. Chen, S.-S. Wang, X. Lu, Y. Tsao, and C.-H. Lee, "A Deep Denoising Autoencoder Approach to Improving the Intelligibility of Voded Speech in Cochlear Implant Simulation," *IEEE Transactions on Biomedical Engineering*, 2016.
- [11] F. Chen, Y. Hu, and M. Yuan, "Evaluation of noise reduction methods for sentence recognition by Mandarin-speaking cochlear implant listeners," *Ear and Hearing*, vol. 36, no.1, pp. 61-71, 2015.
- [12] J. Chen, "Fundamentals of Noise Reduction," in *Spring Handbook of Speech Processing*, Springer, 2008, ch. 43.
- [13] P. Scalart and J. V. Filho, "Speech enhancement based on a priori signal to noise estimation," in *Proc. ICASSP*, 1996, pp. 629-632, 1996.
- [14] Y. Ephraim and D. Malah, "Speech enhancement using a minimum mean-square error short-time spectral amplitude estimator," *IEEE Transactions on Acoustics, Speech and Signal Processing*, vol. 32, pp. 1109-1121, 1984.
- [15] R. Martin, "Speech enhancement based on minimum mean-square error estimation and supergaussian priors," *IEEE Transactions on Speech and Audio Processing*, vol. 13, pp. 845-856, 2005.
- [16] Y. Tsao and Y.-H. Lai, "Generalized maximum a posteriori spectral amplitude estimation for speech enhancement," *Speech Communication*, vol. 76, 2015.
- [17] X. Lu, Y. Tsao, S. Matsuda, and C. Hori, "Speech enhancement based on deep denoising autoencoder," in *Proc. INTERSPEECH*, 2013, pp. 436-440.
- [18] X. Lu, Y. Tsao, S. Matsuda, and C. Hori, "Ensemble modeling of denoising autoencoder for speech spectrum restoration," in *Proc. INTERSPEECH*, 2014, pp. 885-889.
- [19] Y. Xu, J. Du, L.-R. Dai, and C.-H. Lee, "An experimental study on speech enhancement based on deep neural networks," *IEEE Signal Processing Letters*, vol. 21, pp. 65-68, 2014.
- [20] D. Liu, P. Smaragdis, and M. Kim, "Experiments on deep learning for speech denoising," in *Proc. INTERSPEECH*, 2014, pp. 2685-2689.
- [21] S.-W. Fu, Y. Tsao, and X. Lu, "SNR-Aware Convolutional Neural Network Modeling for Speech Enhancement," in *Proc. INTERSPEECH*, 2016.
- [22] M. Zhao, D. Wang, Z. Zhang, and X. Zhang, "Music removal by denoising autoencoder in speech recognition," in *Proc. APSIPA*, 2015.
- [23] H. McGurk and J. MacDonald, "Hearing lips and seeing voices," *Nature*, vol. 264, pp. 746-748, 1976.
- [24] D. G. Stork and M. E. Hennecke, *Speechreading by Humans and Machines*, Springer, 1996.
- [25] G. Potamianos, C. Neti, G. Gravier, A. Garg, and Andrew W, "Recent Advances in the Automatic Recognition of Audio-Visual Speech," *Proceedings of IEEE*, vol. 91, no. 9, 2003.
- [26] D. Kolossa, S. Zeiler, A. Vorwerk, and R. Orglmeister, "Audio-visual Speech Recognition with Missing or Unreliable Data," in *Proc. AVSP*, 2009, pp. 117-122.
- [27] A. V. Nefian, L. Liang, X. Pi, X. Liu, and K. Murphy, "Dynamic Bayesian Networks for Audio-Visual Speech Recognition," *EURASIP Journal on Applied Signal Processing*, vol. 2002, no. 11, pp.1274-1288, 2002.
- [28] A. H. Abdelaziz, S. Zeiler, and D. Kolossa, "Twin-HMM-based audio-visual speech enhancement," in *Proc. ICASSP*, 2013, pp. 3726-3730.
- [29] J.-C. Hou, S.-S. Wang, Y.-H. Lai, J.-C. Lin, Y. Tsao, H.-W. Chang, and H.-M. Wang, "Audio-Visual Speech Enhancement using Deep Neural Networks," in *Proc. APSIPA*, 2016.
- [30] G. Tzimiropoulos and M. Pantic, "Gauss-Newton Deformable Part Models for Face Alignment in-the-Wild," in *Proc. CVPR*, 2014, pp. 1851-1858.
- [31] Z. Wu, S. Sivasadas, Y. K. Tan, M. Bin, and R. S. M. Goh, "Multi-Modal Hybrid Deep Neural Network for Speech Enhancement," *arXiv preprint arXiv:1606.04750*, 2016.
- [32] A. W. Rix, J. G. Beerends, M. P. Hollier, and A. P. Hekstra, "Perceptual evaluation of speech quality (PESQ) – a new method for speech quality assessment of telephone networks and codecs," in *Proc. ICASSP*, 2001.
- [33] C. Taal, R. Hendriks, R. Heusdens, and J. Jensen, "An Algorithm for Intelligibility Prediction of Time-Frequency Weighted Noisy Speech," *IEEE Transactions on Acoustics, Speech and Signal Processing*, vol. 19, pp. 2125-2136, 2011.
- [34] J. Chen, J. Benesty, Y. Huang, and S. Doclo, "New insights into the noise reduction Wiener filter," *IEEE/ACM Transactions on Audio, Speech, and Language Processing*, vol. 14, pp. 1218-1234, 2006.
- [35] J. M. Kates and K. H. Arehart, "The Hearing-Aid Speech Quality Index (HASQI)," *Journal of the Audio Engineering Society*, vol. 58, no. 5, pp. 363-381, 2010.
- [36] J. M. Kates and K. H. Arehart, "The Hearing-Aid Speech Perception index (HASPI)," *Speech Communication*, vol. 65, pp. 75-93, 2014.
- [37] P. Viola and M. J. Jones, "Robust Real-Time Face Detection," *International Journal of Computer Vision*, vol. 57, no. 2, pp. 137-154, 2004.
- [38] ITU-R, "Relative timing of sound and vision for broadcasting", Rec. Bt.1359, 1998.
- [39] D. Kingma and J. Ba, "Adam: A method for stochastic optimization," *arXiv preprint arXiv:1412.6980*, 2014.